

Article

Analysis of Spatial Variability of Plough Layer Compaction by High-Power and No-Tillage Multifunction Units in Northeast China

Wenjie Li ^{1,2}, Zhenghe Song ^{1,2}, Minli Yang ^{1,3}, Xiao Yang ^{1,2,*} , Zhenhao Luo ^{1,2} and Weijie Guo ^{1,2}¹ College of Engineering, China Agricultural University, Beijing 100083, China² Beijing Key Laboratory of Optimized Design for Modern Agricultural Equipment, Beijing 100083, China³ China Research Center for Agricultural Mechanization Development, China Agricultural University, Beijing 100083, China

* Correspondence: yangxiao2020@cau.edu.cn

Abstract: In this study, we addressed the problem of the spatial variability of plough layer compaction by high-power and no-tillage multifunction units in the management of maize planting in the Great Northern Wilderness in China. A comprehensive field experiment involving high-power and no-tillage multifunction units for 165 acres of maize was conducted and analyzed using GIS. Firstly, the test area was divided into four areas, and points were set at equal horizontal distances to collect data on the compactness, water content, porosity and fatigue of the plough layer at different depths. Secondly, the GIS kriging difference method was used to analyze the impact of longitudinal compaction of the plough layer profile at each depth in different test areas. Thirdly, the GIS kriging difference method was used to analyze the lateral spatial distribution of plough layer compaction. Finally, the spatial longitudinal and transverse variabilities of the plough layer were summarized, and the effect of the high-power and no-tillage multifunction units on the physical ecology of the soil in the plough layer was investigated. The results show that the physical properties of the plough layer can be significantly affected by compaction after spreading in the middle tillage period. The surface soil was most affected, with the greatest change in compactness and porosity; the rate of change of soil compactness reached 143.49% and the rate of change of soil porosity reached 40.57%. With the increase in soil depth, the rate of change of soil compactness and porosity gradually decreased. The greatest variation in soil moisture content was found in the middle layer and reached a maximum of 13.78% at a depth of approximately 20 cm. The results of the spatial variability analysis show that the mean values of $c_0/(c_0 + c)$ for the spatial semi-variance functions of compactness, water content and porosity of the tilled soil in the longitudinal space of each test area before compaction were approximately 15%, 19% and 20%, respectively; after compaction, the mean values were approximately 33%, 23% and 30%, respectively; the mean values of $c_0/(c_0 + c)$ for the spatial semi-variance functions of compactness, water content and porosity change of the tilled soil were approximately 24%, 14% and 12%, respectively. The mean values of $c_0/(c_0 + c)$ for the spatial semi-variance functions of compactness, water content and porosity of the soil at each depth in the lateral space before compaction were approximately 80%, 71% and 78%, respectively, and after compaction the mean values were approximately 40%, 23% and 24%, respectively, with the mean values of $c_0/(c_0 + c)$ along the east–west direction being approximately 8%, 27% and 18%, and the mean values of $c_0/(c_0 + c)$ along the north–south direction being approximately 9%, 0% and 20%. The results show that compaction by high-power and no-tillage multifunction units led to a decrease in the spatial variability of soil physical parameters at each depth of tillage in the black soil layer in the longitudinal space, while the spatial variability of the soil physical parameters at each depth of tillage in the black soil layer in the transverse space increased. Moreover, the degree of influence of compaction by high-power and no-tillage multifunction units on soil physical parameters was higher in both vertical and horizontal spaces. This study can provide a theoretical reference for the analysis of the impact of large units on the compaction of black soil layers from the perspective of GIS.



Citation: Li, W.; Song, Z.; Yang, M.; Yang, X.; Luo, Z.; Guo, W. Analysis of Spatial Variability of Plough Layer Compaction by High-Power and No-Tillage Multifunction Units in Northeast China. *Agriculture* **2022**, *12*, 1530. <https://doi.org/10.3390/agriculture12101530>

Academic Editor: Massimo Cecchini

Received: 26 August 2022

Accepted: 21 September 2022

Published: 23 September 2022

Publisher's Note: MDPI stays neutral with regard to jurisdictional claims in published maps and institutional affiliations.



Copyright: © 2022 by the authors. Licensee MDPI, Basel, Switzerland. This article is an open access article distributed under the terms and conditions of the Creative Commons Attribution (CC BY) license (<https://creativecommons.org/licenses/by/4.0/>).

Keywords: plough layer compaction; spatial variability; GIS model; high-power and no-tillage multifunction units; black land conservation

1. Introduction

A no-till planter has the versatility to protect the soil environment and the maize planting process, with seeding, fertilizer spreading and mid-tillage all being achieved with no-till planters in the maize planting process in Northeast China. Three heavy-duty no-till units are required for maize field management on Tsimshatsui farms throughout the year, which in total equates to 36t of heavy-duty units causing severe tillage compaction on black soil with low organic matter that is otherwise resistant to shear and compaction. In this study, a representative mid-tillage session was therefore selected for the trial test.

Currently, the mechanization of agricultural production is increasing in northeast China, but it also creates many problems, such as the soil compaction effects caused by heavy agricultural machinery [1–3]. While improving labor efficiency, high-power agricultural machinery can have lasting compaction effects on field soils, hindering the growth of crop roots and the normal operation of tillage implements, and even leading to black land degradation. No-till seeders are often used as fertilizer spreaders on northeastern farms, achieving a combination of mid-tillage and fertilizer spreading, and the units therefore have a compaction effect on the tilled soil. Analysis of tillage compaction mechanisms has positive significance for black land conservation.

Since the 1950s, scientific researchers in the United States, the United Kingdom and other developed agricultural countries have been conducting systematic research on soil compaction mechanisms, mechanical models and compaction hazards. They have made some achievements in the process of mechanical soil compaction in agricultural fields and formed a system of technical measures by which to reduce mechanical soil compaction in soil tillage technology [1].

Soil compaction has been studied by scholars using a variety of methods, mainly focusing on soil properties. Wang et al. [2] used field trials to investigate the effects of multiple transfers of stress from different types of tractors on soil capacity and crop growth. Their study showed that the effect of different tractor load compaction on maize yield increased significantly with an increasing number of compaction passes. Qiang et al. [3] explored the effects of deep loosening and opening measures on the construction of soil tillage layers and the yield and water use efficiency of winter wheat in the North China Plain, and showed that deep loosening could better reconcile water consumption and yield. Acquah et al. [4] studied the effect of traffic on sandy loam soils in three tillage systems in a field trial and showed that the no-till system had higher values for all soil characteristics compared to disc and spring tine tillage systems. Orzech et al. [5] studied the effects of compaction and different tillage methods on soil bulk density and water content. The results of their experiment showed that spring barley yields were higher in the compaction treatment, while the opposite was true for winter wheat. Moitzi et al. [6] used a three-factor research design in a field trial and the results showed that tire inflation pressure and ground cover had a significant effect on the measured parameters. Based on the analysis of the global adoption rate and benefits of deep pine technology and the current application status of deep pine machines, Lou et al. [7] reviewed the research methods, technical features and development trends of deep-hole machines from five key aspects, including deep sand shovel design, drag resistance technology, tillage depth detection and control technology, and soil mechanics interaction research.

Some scholars have also conducted studies using models. Fu et al. [8] proposed a new and improved model to simulate the soil compaction process based on the original compaction model. Foreign researchers have mainly studied soil compaction with the help of models. For example, Keller et al. [9] used the Soilflex model to input agricultural machinery and soil parameters and output soil stress–strain relationships to reflect soil compaction.

Castioni Guilherme A.F. et al. [10] used the SoilFlex model to simulate the contact area of tires and the stress transferred to the soil during straw removal. Obour P. B et al. [11] showed that soil hydraulic properties may be a more sensitive indicator of the effect of soil compaction on soil structure and pore system function. Faloye O. T et al. [12] collected soil samples in two sampling directions and at four depths, and in-situ soil samples were collected at three different locations, demonstrating that the pore water pressure may remain constant or decrease with the increase in the medium and coarse pore fractions within the soil. The smaller the pore connectivity and continuity, the smaller the negative variation of pore water pressure.

With the wide application of technologies such as remote sensing (RS) and geographic information systems (GISs), the spatial dynamics of land use and landscape patterns have been studied increasingly intensively [13]. Yang W et al. [14] used GIS technology and empirical research to measure and evaluate the suitability of land for industrial transfer, which provides a methodological reference and practical support for the rational development, utilization and management of land resources on low hills and gentle slopes. Sun H et al. [15] used RS, GIS technology and landscape ecology to analyze the spatial and temporal changes in land use and landscape patterns in their study area. Liu D et al. [16] used GIS spatial analysis technology to create a fine-grid projection of zoning indexes, which provided some scientific basis for the reasonable planting of *Dendrobium ferruginum* in Yunnan Province. Houyun S. et al. [17] explored the degree of soil heavy-metal ecological risk accumulation and its influencing factors in a watershed in Chengde City based on a redundancy analysis of land use types and a GIS baseline partitioning model. In that study, the ranking of the strengths and weaknesses of various heavy metal accumulation degrees in the surface soils of the study area was completed. Bernadette J et al. [18] used ArcGIS software for secondary data representation to study the maximum depletion zone of groundwater in the KMC area. The Department of Soil and Water in the Faculty of Agriculture at Benha University used AHP and GIS geospatial techniques for the land degradation vulnerability mapping of newly reclaimed desert oases in hyper-arid agroecosystems [19]. Zhang Y et al. [20] chose part of Mianzhu city in the transition zone between Longmen Mountains and Chengdu Plain as their study area, and used various methods to spatially interpolate soil moisture based on soil sampling and testing to obtain soil moisture data based on GIS technology. They used soil sample point moisture data as reference values with which to compare and analyze their interpolation results. Liu Y et al. [21] made a dynamic prediction of soil moisture changes in a future time period and introduced RS and GIS spatial technologies to obtain important forecast model parameters such as vegetation type, albedo, vegetation cover and soil texture in Beijing at the time of forecasting, initially realizing the visualization of soil moisture forecasting in the spatial range of Beijing.

In previous studies on agricultural soils, most of the parameters such as soil compactness and moisture content were expressed in the form of curve graphs, which were not intuitive enough. Most of the studies were also based on small areas of farmland and had too few sampling points. In the study presented in this paper, the interpolation method was used to express the soil physical parameters of the farmland as a whole, which allows for a more intuitive and accurate representation of the soil state in all areas of the farmland while minimizing the experimental workload. We analyzed the spatial variability of the compactness, moisture content and porosity of the soil in the field, based on GIS geographic information analysis, and finally analyzed the effect of a heavy-duty fertilizer-spreading unit on the spatial variability of the soil physical parameters in the cultivated layer.

2. Materials and Methods

2.1. Overview of the Experimental Area

The study was carried out in Plots 1–3 (125°30' E, 48°54' N), Zone 3, Jianshan Farm, Jiusan Administration, the Great Northern Wilderness, China. This area has a cold-temperate continental monsoon climate with an average annual temperature of $-4\sim 5$ °C. High summer temperatures, high precipitation and long light hours make it suitable for the growth

of corn and other crops. Solar radiation is abundant, and the annual sunshine hours are generally in the range of 2300~2800 h. As shown in Figure 1, the test area is a large-scale continuous maize farmland with a rectangular shape, measuring 1.5 km × 0.46 km. The heavy-duty fertilizer-spreading unit comprises a heavy-duty tractor of 220 hp (the main parameters of the tractor are shown in Table 1) and a supporting 6.1 m wide no-till planter, and the tires used are ultra-low-pressure radial tires (the main parameters of the tires are shown in Table 1). The unit has an average operating speed of 10 km/h and a total unit weight of about 12 tons when fully loaded.



Figure 1. Overview of the experimental area.

Table 1. Seeding unit parameters.

Tractor	Number of Engine Cylinders	Power Rating	Operating Speed Range	Length × Width × Height	Overall Vehicle Mass
	6	150.8 kW	1600–2100 r/min	5.5 × 2.44 × 3.18 m	7770 kg
Tire	Position	Specification	Wheel Diameter	Tire Pressure	Grounding Area
	Front	420/90 R30	762.00 mm	140 kPa	2522 cm ²
	Rear	480/80 R46	1168.4 mm	200 kPa	3234 cm ²
No-Till Seeders	Working Width	Weight	Capacity	Matching Power	Trencher Ground Clearance
	6.1 m	6500 kg	405 L/m	104 kW	20.3 cm

2.2. Experimental Scheme

The study was conducted in June 2021, Figure 2 shows the test site, and for the convenience of conducting the experiment and data analysis, the test area of 165 acres was divided into 4 plots. Each plot had several ruts, and the rutted furrows with incomplete rutting marks were removed, 15 monopoly furrows were selected for each plot, 10 test points were selected for each monopoly furrow to measure soil moisture content and soil compactness, and then 10 sampling points were selected from which to take soil samples with a ring knife to measure the degree of soil porosity. The average value of all test points was used to represent the soil compactness, soil moisture content and porosity. The soil compactness, soil moisture content and porosity of each point were measured before and

after the unit operation. A questionnaire was used to determine the overall perception of operator fatigue during tractor operation.



Figure 2. Tire deformation and ground contact area.

3. Results

Descriptive Analysis of Physical Parameters of Cultivated Soils after Operation of High-Power and No-Tillage Multifunction Units

As can be seen from Table 2, the surface soil in the test area was most affected by compaction. The maximum compactness of the surface plough layer reached 2050.13 kPa and the minimum compactness was 1595.86 kPa after the unit operation, with the change rate at 2.11~143.49%. The porosity of the surface soil was most affected by compaction; the maximum porosity of the surface plough layer was 15.04%, and the minimum porosity was 7.96%, with a variation rate of 14.92~40.57%. The water content of the plough layer at the depth of 20~30 cm was most affected by compaction, with a maximum water content of 24.10% and a minimum water content of 19.88% after the unit operation, with a variation rate of 5.86~13.78%.

Table 2. Soil parameters of plough layer before and after compaction in each test area.

Test Area	Soil Depth (cm)	Soil Compactness			Soil Water Content			Soil Porosity		
		Before (kPa)	After (kPa)	Rate of Change (%)	Before (kPa)	After (kPa)	Rate of Change (%)	Before (kPa)	After (kPa)	Rate of Change (%)
I	5	888.23	1595.86	79.67	21.92	20.61	5.98	20.92	14.96	28.49
	10	1343.75	1918.38	42.76	22.57	21.23	5.94	18.37	14.87	19.05
	15	1943.87	2418.23	24.40	23.44	21.74	7.25	14.63	12.34	15.65
	20	2588.91	3078.72	18.95	24.84	22.11	10.99	13.02	10.27	21.12
	30	4640.66	4738.58	2.11	25.39	23.41	7.80	11.46	9.75	14.92
II	5	836.61	1848.91	121.56	22.06	20.58	6.69	21.11	13.24	37.28
	10	1348.08	2236.46	65.97	22.69	21.03	7.33	19.35	13.47	30.37
	15	2066.49	2893.09	40.00	23.93	21.23	11.30	15.61	11.17	28.47
	20	2667.47	3200.96	20.24	25.09	21.81	13.05	13.11	8.98	31.51
	30	4524.26	4886.20	8.36	25.84	23.27	9.94	11.89	8.70	26.79

Table 2. Cont.

Test Area	Soil Depth (cm)	Soil Compactness			Soil Water Content			Soil Porosity		
		Before (kPa)	After (kPa)	Rate of Change (%)	Before (kPa)	After (kPa)	Rate of Change (%)	Before (kPa)	After (kPa)	Rate of Change (%)
III	5	721.38	1428.33	98.41	21.83	20.65	5.39	20.86	15.04	27.87
	10	1312.20	1968.30	50.30	22.52	21.20	5.86	19.32	14.56	24.66
	15	1941.38	2407.31	23.97	24.07	21.69	9.86	15.71	12.34	21.45
	20	2066.49	2500.45	21.31	25.28	22.44	11.25	13.07	10.02	23.34
	30	4589.72	4865.10	6.20	26.35	24.10	8.55	11.62	9.58	17.65
IV	5	841.96	2050.13	143.49	21.68	20.28	8.30	21.62	12.85	40.57
	10	1317.12	2370.86	80.00	23.39	19.88	9.16	19.61	12.62	35.64
	15	2037.74	2863.22	40.51	23.61	20.78	11.99	15.88	10.37	34.69
	20	2854.82	3602.82	26.20	24.96	21.52	13.78	13.21	8.18	38.06
	30	4563.73	5173.30	13.36	25.92	23.31	10.07	11.71	7.96	32.22

From Table 2, it can also be seen that with the increase in soil depth, the compactness of plough-layer soil gradually increases, but the relative change rate of compactness gradually decreases. With the increase in soil depth, the soil porosity of the plough layer and its change rate gradually decreases. With the increase in soil depth, the change in water content is not obvious, but the water content of the plough layer at a depth of 20~30 cm depth is affected by compaction, and the maximum change rate is 13.78%.

4. Discussion

4.1. Basic Concepts of GIS Systems

A geographic information system (GIS) is a computerized spatial or spatio-temporal information system for the representation, acquisition, processing, management, analysis and application of characteristic elements of geospatial entities and phenomena; the random fields estimated by the kriging method of difference are taken at sample points in agreement with the corresponding observations, and are widely used for the spatial interpolation of various types of observations, such as the sampling of groundwater levels and soil moisture in geology; environmental science research in atmospheric pollution and soil contaminants in environmental science research; and single-point observations of near-surface wind fields, air temperature, precipitation, etc., in atmospheric science.

In this study, we combined soil data from 600 test sites obtained from our experiment to first plot soil compactness, moisture content and porosity data at various depths of the farmland before the unit operation, and then interpolated the samples based on the ordinary kriging method using some of the test site data after the unit operation as samples to produce a cloud map of different tillage parameters of the soil in the test area. Figure 3 shows the longitudinal profile cloud diagram of soil compactness and the rate of change before and after compaction in each test area. It can be seen that before compaction of the plough layer in the whole test area, about 10 cm and 20 cm deep, three compactness zones were formed. After the fertilizer-spreading operation, the compactness of each zone increased significantly; the rate of change can reflect to a certain extent the strength of the action of the fertilizer-spreading unit on the compaction of the plough layer. This may be due to the fact that the stress transmission amplitude of compaction is weakened by the shallow soil and that agronomic links such as deep pine make the soil in the test area more uniform. Therefore, after the compaction of the plough layer by the fertilizer-spreading unit, the longitudinal spatial variability of the compactness of the plough layer at each depth was high and the distribution showed non-uniformity; however, the longitudinal effect of compaction on the distribution of compactness became uniform.

4.2. Principle of the Kriging Method

4.2.1. Basic Theory of the Kriging Method

The core idea of kriging interpolation is that the variability of property values at two points is positively correlated with the distance between them within a certain distance. Applying this idea to our study, we can consider that the soil parameter value $Z^*(x_0)$ at a

point in an agricultural field within a certain distance is a weighted sum of the measured soil data $Z(x_i)$ around this point, i.e.,

$$Z^*(x_0) = \sum_{i=1}^N \lambda_i Z(x_i) \tag{1}$$

where N is the number of points that can determine the soil parameter value at that point; $Z^*(x_0)$ is the band estimate soil parameter value at point x_0 in the farm field; $Z(x_i)$ represents the soil parameter value at the i -th known point; and λ_i represents the weighting factor for the i -th known point.

To obtain the most accurate results possible, two assumptions are made:

(1) λ_i should be such that the difference between the estimated value $Z^*(x_0)$ and the true value $Z(x_0)$ at point x_0 is minimized, and also that the variance of the difference between the two is as small as possible, i.e.,

$$E[Z^*(x_0) - Z(x_0)] = 0 \tag{2}$$

$$\min\{\text{Var}[Z^*(x_0) - Z(x_0)]\} \tag{3}$$

(2) The space is smooth and the value $Z = Z(x,y)$ at any point in the space is given by the regional mean c and the attendant deviation $R(x,y)$, where the variances of the deviations are all constants, i.e.,

$$Z(x,y) = R(x,y) + c \tag{4}$$

$$\text{Var}[R(x,y)] = \sigma^2 \tag{5}$$

Written in the expected form, we have

$$E(z) = c \tag{6}$$

The above two assumptions make it feasible to estimate unknown-point soil parameter values from known-point soil parameter values in an agricultural field. Using Equation (3) as the objective function and optimizing it gives

$$\begin{bmatrix} \lambda_1 \\ \lambda_2 \\ \vdots \\ \lambda_n \\ \lambda_m \end{bmatrix} = \begin{bmatrix} \gamma_{11} & \gamma_{12} & \cdots & \gamma_{1n} & 1 \\ \gamma_{21} & \gamma_{22} & \cdots & \gamma_{2n} & 1 \\ \vdots & \vdots & \dots & \vdots & \vdots \\ \gamma_{n1} & \gamma_{n2} & \cdots & \gamma_{nn} & 1 \\ 1 & 1 & \cdots & 1 & 0 \end{bmatrix}^{-1} \begin{bmatrix} \gamma(x_1, x_0) \\ \gamma(x_2, x_0) \\ \vdots \\ \gamma(x_n, x_0) \\ 1 \end{bmatrix} \tag{7}$$

where $\gamma(x_i, x_j)$ denotes the semi-variance between the two neighborhood points x_i and x_j , λ is a constant and the 0-th neighborhood point denotes the point to be found.

$$\gamma_{ij} = \frac{[Z(x_i) - Z(x_j)]^2}{2} \tag{8}$$

The multi-group distance can be found using Equation (8); this is the semi-covariance relationship $[d(x_i, x_j), \gamma(x_i, x_j)]$, where $d_{ij}(x_i, x_j)$ denotes two test points between the distance; we choose a suitable functional form, and obtain the resulting multi-group distance. The semi-covariance relationship will be fitted to the function $\gamma = f(d)$. Because the location of the point to be sought is known, $d(x_1, x_0)$ can be found, which will be brought into the function to obtain $\gamma(x_1, x_0), \dots, \gamma(x_n, x_0)$. At this point, it will be possible to solve Matrix (7) of all points in the weight coefficient λ .

4.2.2. Semi-Variable Function Theoretical Model

As mentioned in the previous section, it is necessary to choose a suitable functional form to fit the resulting multi-group distance-semi-variance relationship to the function $\gamma = f(d)$. According to the core idea of kriging interpolation, the value of γ increases with distance within a certain distance, and γ tends to stabilize when this distance is exceeded. We call this function the semi-variance function. The semi-variance function is used to represent the spatial correlation; it can be used to describe the relationship between the semi-variance value γ and the distance d . Commonly used semi-variance model functions are spherical functions, exponential functions, Gaussian functions, etc. The spherical model is the most widely used theoretical model in geostatistical analysis. Many regionalized variables of the theoretical model can be used to fit the model, so we used a spherical model. The expression of the model is as follows

$$\gamma(h) = \begin{cases} c_0 & h = 0 \\ c_0 + c \left(\frac{3h}{2a} - \frac{h^3}{2a^3} \right) & 0 < h \leq a \\ c_0 + c & h > a \end{cases} \quad (9)$$

where c_0 is the block gold value; c is the offset abutment value; $c_0 + c$ is the abutment value; and a is the spatially dependent range, i.e., the variable range value.

The ratio of the block gold value to the abutment $c_0 / (c_0 + c)$ is used as an indicator of the degree of spatial autocorrelation, and this ratio is related to the degree of spatial correlation as shown in the Table 3.

Table 3. Correspondence table for degree of spatial autocorrelation.

$c_0 / (c_0 + c)$	Degree of Spatial Autocorrelation
<25%	Strong
25–75%	Moderate
>75%	Weak

4.2.3. Maximum Separation Distance and Grouping Step

When calculating the sample semi-variance function cloud map, the first step is to determine the maximum separation distance and grouping step size. The principle of selecting the step size is that the product of the number of groups and the step size is less than half of the maximum distance in all samples. After selecting the appropriate step size, we import the test data into the ArcGIS software, set the appropriate step size and choose to fit the experimental data with a spherical function to produce multiple directional spatial semi-variance functions to check anisotropy.

5. Discussion

5.1. Analysis of Longitudinal Spatial Variability of Physical Parameters in Cultivated Soils

5.1.1. Analysis of the Longitudinal Spatial Semi-Variance Function and Interpolation Results of Soil Compactness in the Cultivated Layer

Soil compaction is an important soil quality indicator. The tractor unit will carry out field operations due to its own mass, the vibration leads to compaction, soil density increases, porosity decreases and water infiltration capacity decreases. This is not conducive to crop root growth, resulting in lower yields, and will make the tillage equipment resistance increase and fuel consumption increase.

As can be seen from Figure 3, the values of $c_0 / (c_0 + c)$ for the longitudinal spatial semi-variance function of soil compactness in each test area before compaction were 16.3%, 15.2%, 14.7% and 16.6%, with strong spatial autocorrelation, while after compaction they were 35.3%, 34.5%, 34.7% and 32.8%, respectively, with moderate spatial autocorrelation. The values of $c_0 / (c_0 + c)$ for the rate of change were 26.2%, 25.7%, 24.9% and 24.1%, respectively, with moderate spatial autocorrelation. Figure 4 shows the longitudinal interpolation of soil

compactness and the rate of change before and after compaction in each test area. This is probably due to the fact that the stress transfer amplitude of compaction was weakened by the shallow soil and that agronomic aspects such as deep pine made the soil in the test area more homogeneous. After compaction of the tillage layer by the fertilizer-spreader unit, the compactness of the surface soil was closer to the compactness of the deep soil layer than before compaction, and the combination of the spatial semi-variance function showed that the longitudinal and deep spatial variability of the compactness of the tillage layer at each depth was reduced.

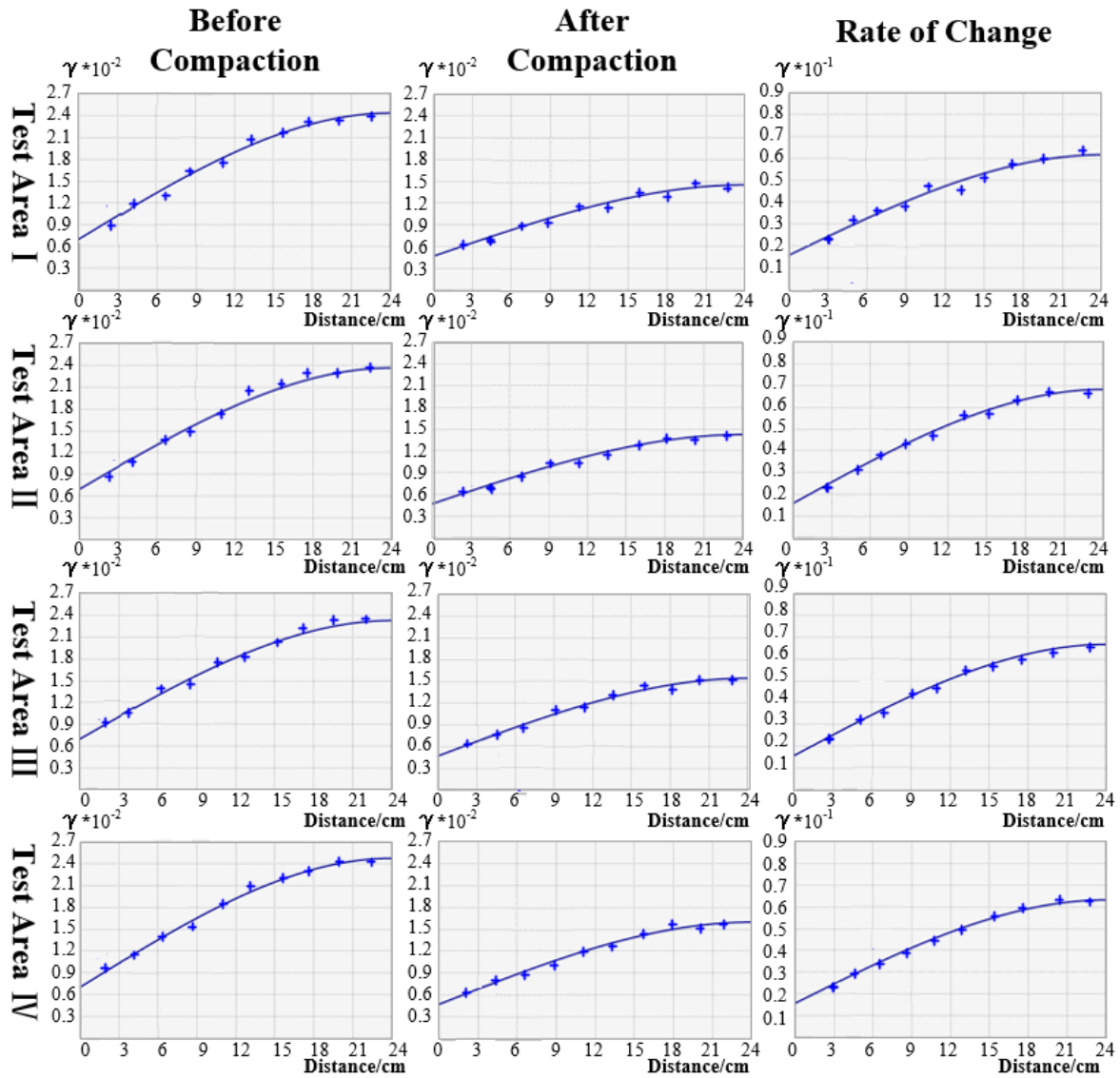


Figure 3. Longitudinal spatial semi–variance function of soil compactness in each test area.

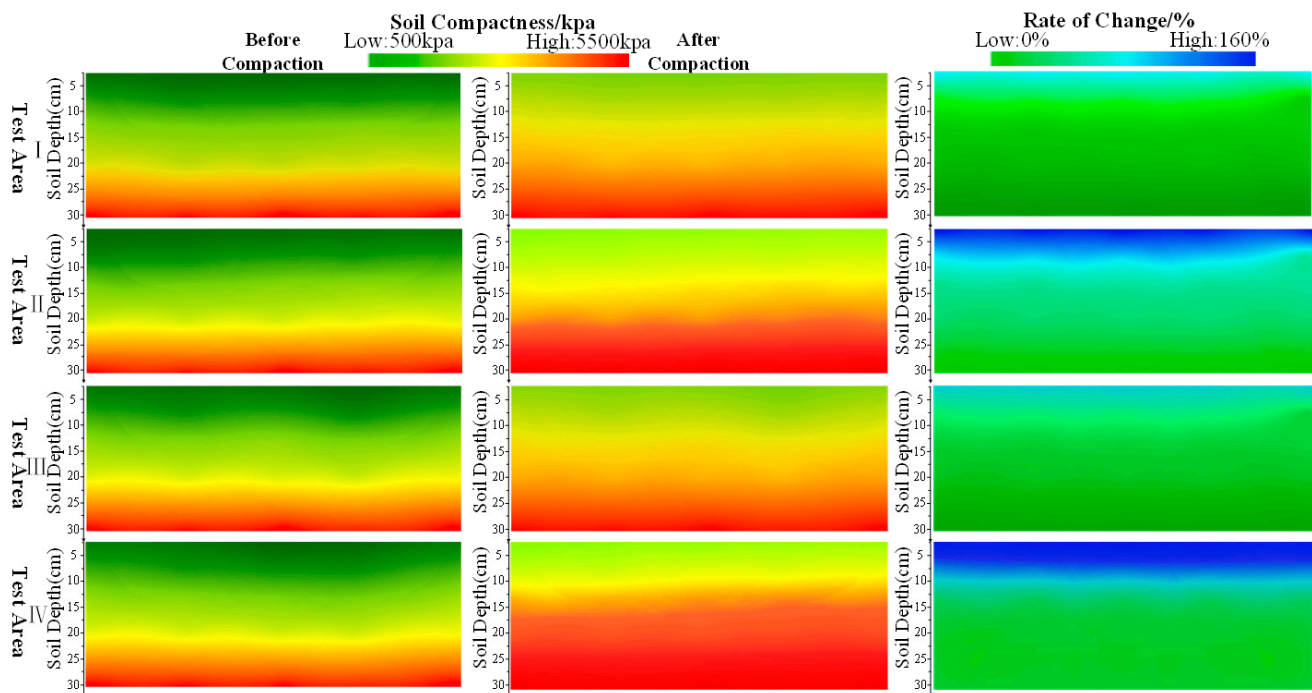


Figure 4. Longitudinal profile clouds of soil compactness before and after compaction in each test area.

5.1.2. Analysis of the Longitudinal Spatial Semi-Variance Function and Interpolation Results of the Water Content of Cultivated Soils

Water content is an important component of soil and is a key source of water for crop growth. Soil water content is given by the percentage of the mass of water in the soil to the overall mass of the soil. When the soil water content is high enough, water and inorganic salts in the soil will enter a plant through the membrane of the plant root system. Too low a soil water content will lead to water shortage in the crop and seriously affect its normal growth.

From Figure 5, it can be seen that the values of $c_0/(c_0 + c)$ of the longitudinal spatial semi-variance function of soil water content in the cultivated layer of each test area before compaction were 18.9%, 19.5%, 20.2% and 19.1%, with strong spatial autocorrelation, and the values of $c_0/(c_0 + c)$ after compaction were 24.5%, 24.7%, 23.6% and 22.1%, respectively, with weaker spatial autocorrelation. The rate of change values of $c_0/(c_0 + c)$ were approximately 14.5%, 13.9%, 15.1% and 14.6%, respectively, with strong spatial autocorrelation. Figure 6 shows the soil water content and rate of change clouds before and after the tractor unit fertilizer-spreading operation in each test area. It can be seen that before the fertilizer-spreading operation, the water content formed two banded areas at a depth of approximately 17.5 cm; after the fertilizer-spreading operation, the water content of each tillage layer decreased and a new banded boundary was formed at a depth of approximately 25 cm, indicating that the propagation of the unit compaction stress can obviously affect the water content up to a depth of 25 cm. The water content of the tillage layer from 10 cm to 25 cm was affected more by compaction, probably because the water content of the tillage layer was larger here and the compaction stress could lead to an obvious reduction in porosity. This is probably due to the fact that by the time the compaction stress propagated to this area, the strength had decayed considerably and was not sufficient to completely compact the pores between the soil particles, resulting in little change in the volumetric water content. In combination with the spatial semi-variance function, the longitudinal spatial variability of the water content of the tillage layer at each depth was reduced after compaction by the fertilizer-spreader unit, as the water content of the soil at depth was

closer to that of the top soil, which remained almost unchanged. The longitudinal effect of compaction on the distribution of water content was also non-uniformly distributed.

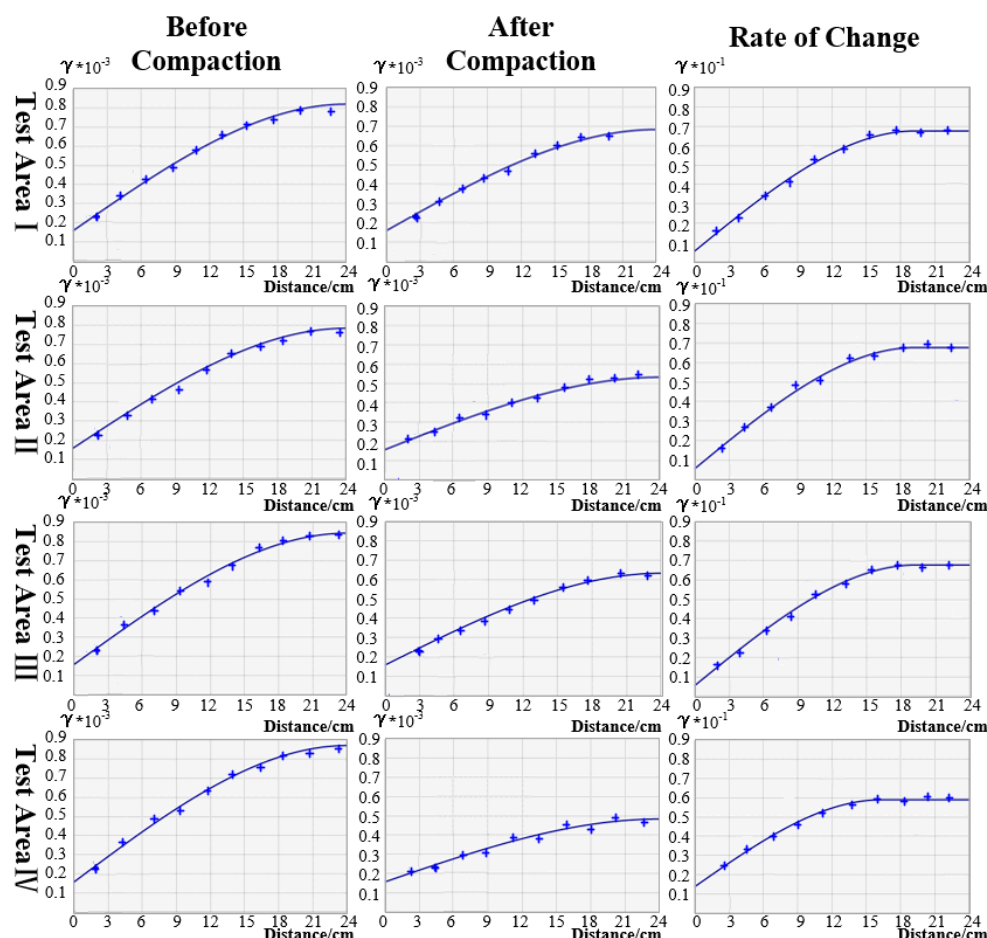


Figure 5. Longitudinal spatial semi-variance function of soil water content in each test area.

5.1.3. Analysis of the Longitudinal Spatial Semi-Variance Function and Interpolation Results of the Porosity of Cultivated Soils

Soil porosity is represented by the percentage of soil pore volume to soil volume; the smaller the soil capacity, the greater the porosity. There are many different shapes of pores within the soil. Water and air flow in the soil through the pore system, which can also store organic matter in the soil. When the soil porosity is too low, it will prevent water, air and organic matter in the soil from entering the plant root system, which will seriously affect the normal growth of the plant root system.

From Figure 7, it can be seen that the values of $c_0/(c_0 + c)$ of the longitudinal spatial semi-variance function of soil porosity in the cultivated layer of each test area before compaction were 19.8%, 20.5%, 20.3% and 22.5%, with strong spatial autocorrelation, while the values of $c_0/(c_0 + c)$ after compaction were 29.6%, 30.5%, 31.2% and 28.9%, respectively, with medium spatial autocorrelation. The rate of change values of $c_0/(c_0 + c)$ were 12.5%, 13.2%, 13.6% and 11.9%, respectively, with strong spatial autocorrelation. Figure 8 shows the soil porosity and the rate of change before and after the operation of the fertilizer-spreading unit in each test area, which shows that before the operation of the spreading unit, two zones were formed at a depth of 15 cm, and the porosity of the shallow layer was higher than that of the deep tillage layer. The porosity of the deeper layers was reduced significantly from 10 cm to 25 cm, and the $c_0/(c_0 + c)$ value of the rate of change was approximately 13%, which was much less than 25%. The variability was reduced.

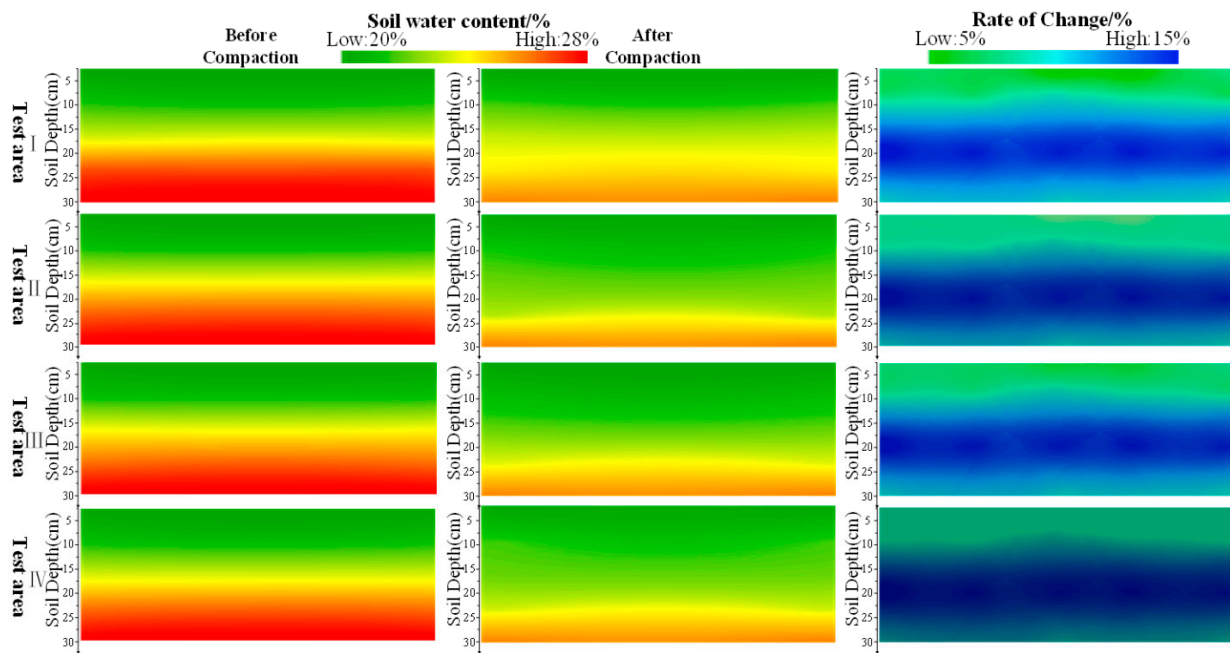


Figure 6. Longitudinal profile clouds of soil moisture content before and after compaction in each test area.

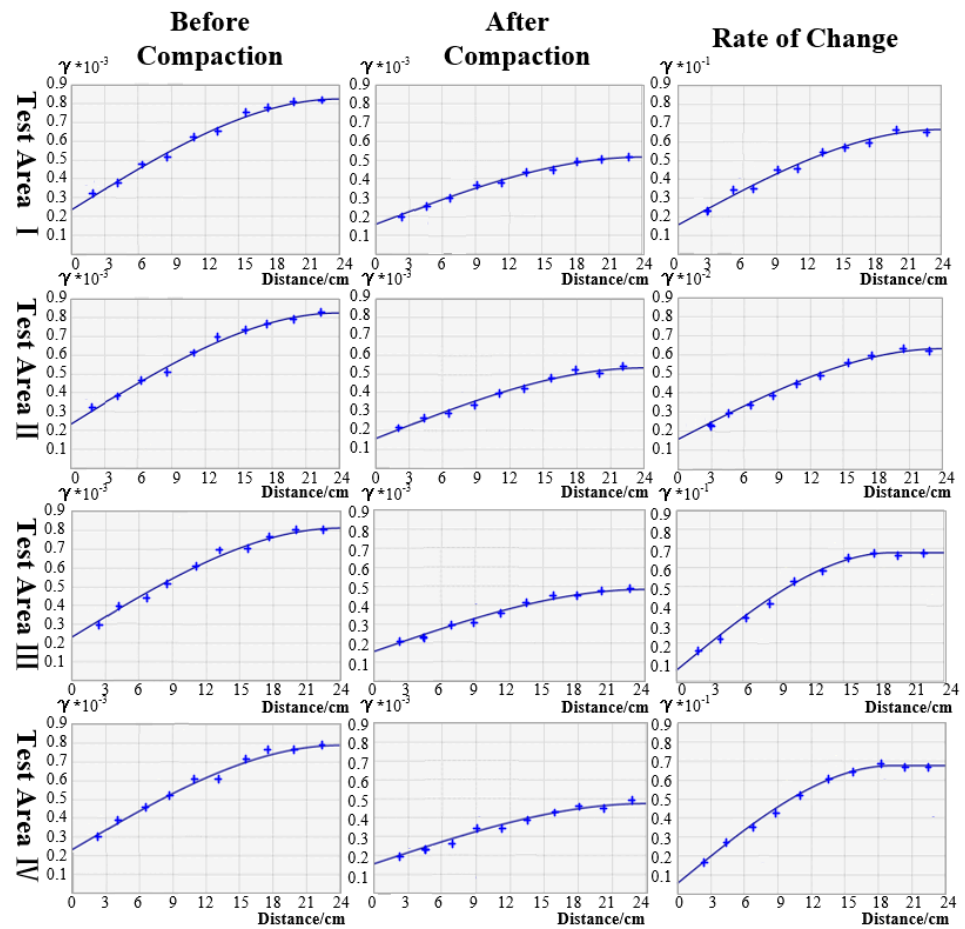


Figure 7. Longitudinal spatial semi-variance function of soil porosity in each test area.

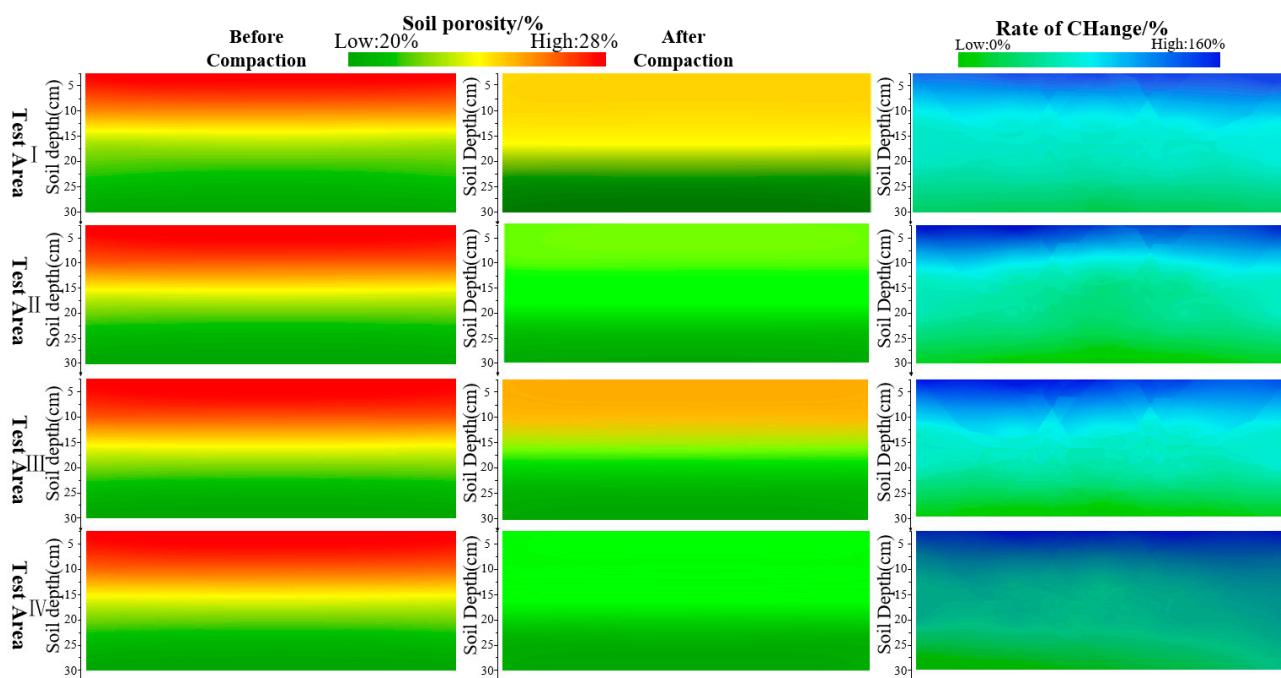


Figure 8. Soil longitudinal porosity clouds before and after compaction in each test area.

5.2. Analysis of the Lateral Spatial Variability of Physical Parameters in Cultivated Soils

5.2.1. The Effect of Tillage Compaction on the Spatial Lateral Variability of Soil Compactness in the Cultivated Layer

The horizontal spatial semi-variance function of the tillage layer at each depth before and after the farming operation was plotted and interpolated. As the quality of the unit changes continuously during the operation of the farm machinery, the variability of the unit in different directions is different. The rate of change of the physical parameters of the soil was used to characterize the effect of the unit on the soil, and the transverse spatial semi-variance function of the rate of change of the soil compactness in the north–south and east–west directions of the tillage layer at each depth was plotted after the operation of the unit to check whether there was a difference in the effect of the unit on the soil in these two directions.

Figure 9 shows the transverse spatial semi-variance function of soil firmness before and after compaction. The ratios of the block gold value to the abutment in the semi-variance function before operation were 77.5%, 75.6%, 80.5% and 82.5%, all of which were greater than 75%, so the spatial autocorrelation of soil firmness before compaction was weak. The ratios of the block gold value to the abutment in the spatial semi-variance function of soil compactness after the unit operation were 39.2%, 40.5%, 42.8% and 43.4%, which were significantly lower than those before the unit operation, with the values of $c_0/(c_0 + c)$ along the east–west direction being 0, 8.7%, 9.1% and 8.6%, respectively, and the values of $c_0/(c_0 + c)$ along the north–south direction being 7.9%, 10.3%, 11.3% and 10.3%, respectively. 10.3%, 11.3% and 10.9% respectively along the north–south direction. It can be seen from Figure 10 that after compaction in the test area, the compactness in the lateral space of the tillage layer at different depths was evenly distributed in a band, and the rate of change clouds were also more even in the lateral space. The compactness in the middle of the maize field was relatively smaller than that in the outer part of the field, which can be attributed to the flat terrain in the middle of the test area and the suitability of the soil for farm machinery. As the depth of the soil increased, the compactness of the soil increased. Areas with greater compactness in the surface soil will also have a correspondingly greater compactness in the depth. After compaction by the tractor unit, the soil compactness at all depths increased significantly, but with the increase in depth, although the compactness of the tillage layer increased, the rate of change gradually weakened, indicating that the

tractor unit operation had a weak effect on the soil compactness at depth. In addition, after compaction by the tractor unit, the soil compactness at all depths was no longer evenly distributed, and the soil compactness gradually decreased from test area 4 to test area 3, and from test area 2 to test area 1. The soil compactness also gradually decreased from test area 4 to test area 3, and from test area 2 to test area 1. However, between test area 3 and test area 2, the soil compactness increased, because the tractor unit first started from test area 4. As the operation continued, the diesel and fertilizer were consumed and the quality of the unit gradually decreased, so the compaction effect of the unit on the soil gradually decreased. This is because the diesel and fertilizer were replenished at the end of test area 3, so the soil compaction increased between test areas 3 and 2. Combined with the semi-variance function analysis, it can be seen that the spatial lateral variability of the soil compactness of the tillage layer increased after the unit operation and was significantly stronger along the east–west direction than along the north–south direction.

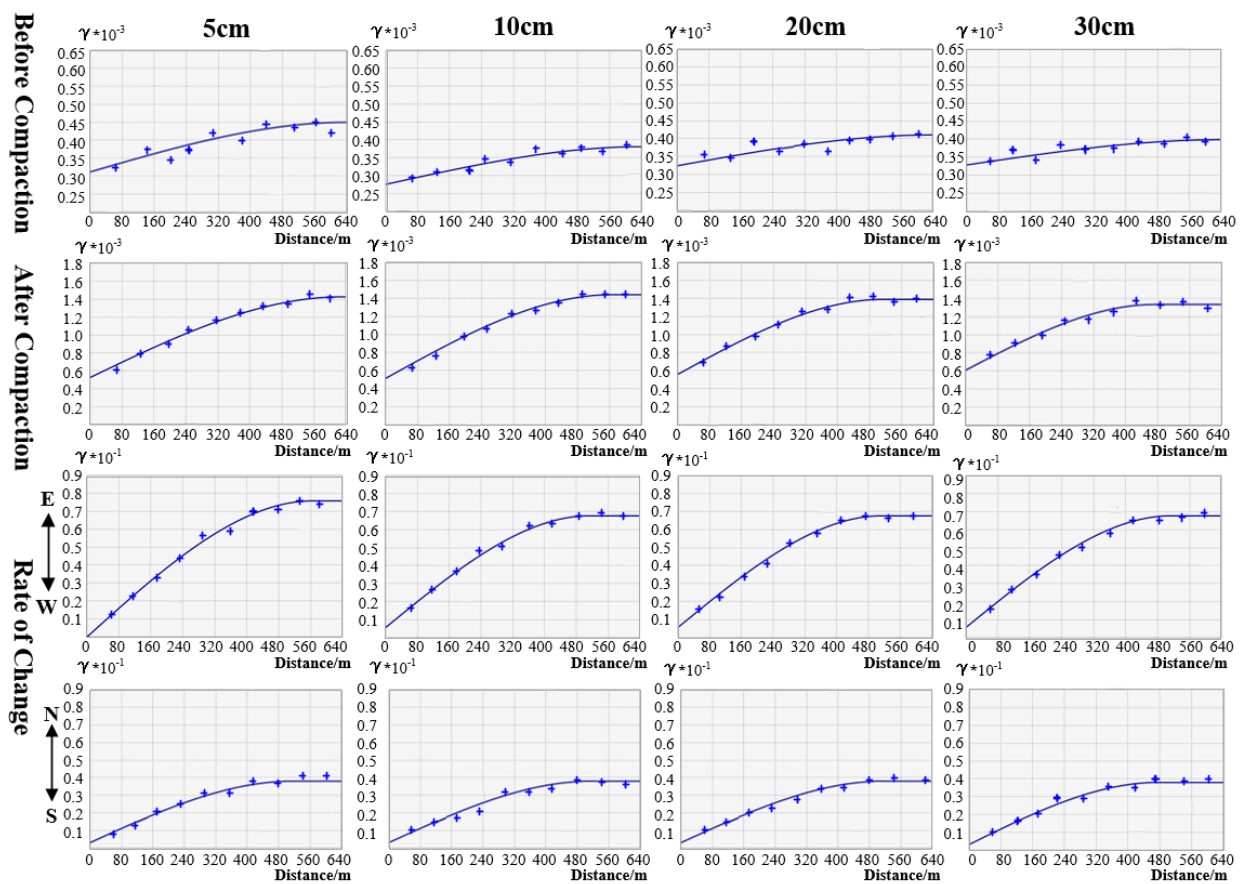


Figure 9. Transverse spatial semi–variance functions for soil compactness at various depths before and after compaction.

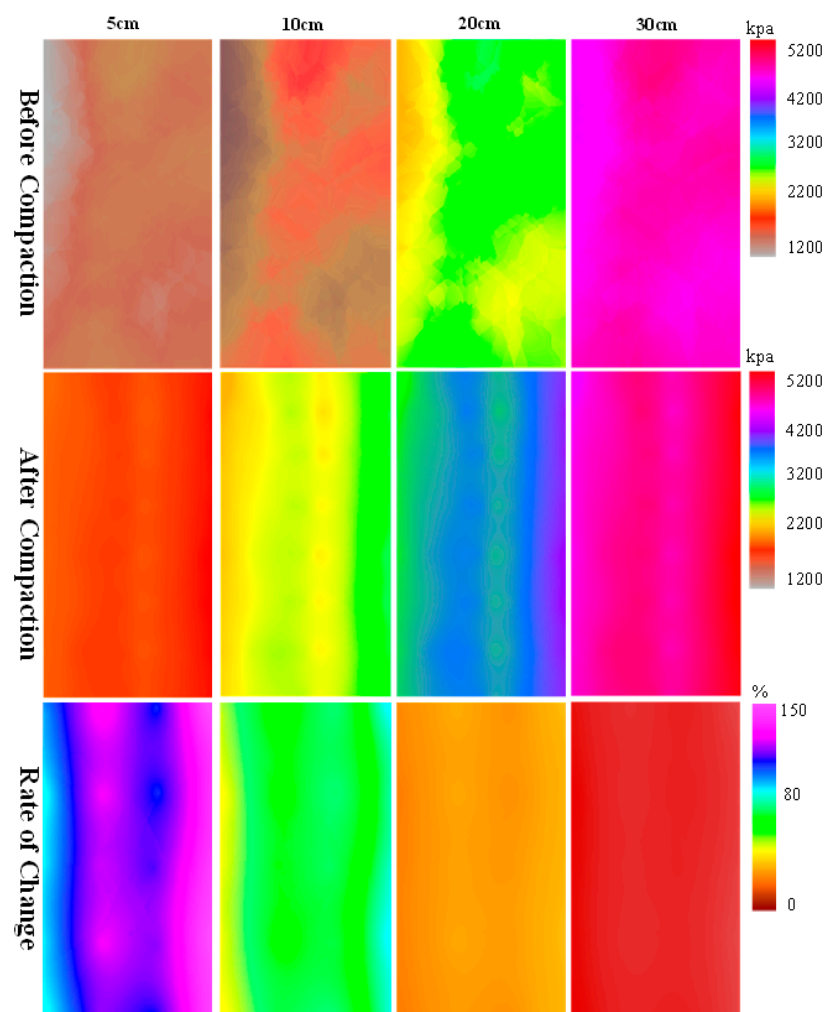


Figure 10. Transverse spatial distribution of soil compactness at each depth before and after compaction.

The literature [1] studied the effect of compaction on the distribution of soil compactness in the longitudinal space, using a method in which the average of experimental data at several depths was expressed in the form of a curve graph; the literature [22] used the form of contour plots to express the variation of soil compactness in the longitudinal space of the soil, and the test results showed that the hardening of the tillage layer caused by soil compaction was mainly concentrated at the depth of 0–30 cm. This is very similar to the results of this study. However, further detailed analysis was not carried out for the 0–30 cm depth of the tillage layer, whereas this study used kriging to interpolate the experimental data for several depths of the tillage layer, which can more accurately express the soil compaction at each depth of the tillage layer. The effect of compaction on soil compaction was analyzed not only from the longitudinal space, but also from the lateral space.

5.2.2. The Effect of Tillage Compaction on the Spatial Lateral Variability of Soil Water Content in the Tillage Layer

Figure 11 shows the transverse spatial semi-variance function of soil moisture content at each depth before and after compaction. The ratios of the block gold value to the abutment $c_0/(c_0 + c)$ in the semi-variance function before operation for each depth of tillage layer were 70.1%, 70.6%, 74.6% and 71.1%, which were less than 75% but very close to 75%, so the spatial autocorrelation of soil moisture content of farmland before compaction was moderate but weak. After the unit operation the ratios of the block gold value to the abutment $c_0/(c_0 + c)$ in the spatial semi-variance function of soil water content in

the tillage layer at each depth were 22.9%, 23.5%, 24.2% and 23.4%, respectively, which were significantly lower than those before the unit operation, among which the values of $c_0/(c_0 + c)$ along the east–west direction were 27.9%, 28.7%, 27.1% and 28.6%, and the values of $c_0/(c_0 + c)$ along the north–south direction were 27.9%, 28.7%, 27.1% and 28.6%, respectively. Figure 12 shows the transverse spatial distribution of soil moisture content in the cultivated layer at each depth before and after compaction, and it can be seen that after compaction, the soil moisture content at each depth was relatively evenly distributed in the transverse space, with slightly larger moisture contents in individual areas. The greater the surface soil moisture content, the greater the deeper soil moisture content compared to other areas, but with the increase in soil depth, the moisture content in each area gradually decreased. The moisture content of the deeper soil was less affected by external influences. After compaction, the water content of the surface soil remained almost unchanged, while at 10 cm and 20 cm the water content of the soil decreased significantly. Therefore, after compaction of the tillage layer by the fertilizer-spreading unit, the lateral spatial variability of the moisture content of the tillage layer at each depth was high and the distribution was non-uniform; the lateral effect of compaction on the distribution of moisture content became non-uniform. Combined with the semi-variance function analysis, it can be seen that the spatial lateral variability of the soil moisture content in the tillage layer increased after the unit operation, and the spatial variability of soil moisture content along the east–west direction was significantly stronger than that along the north–south direction.

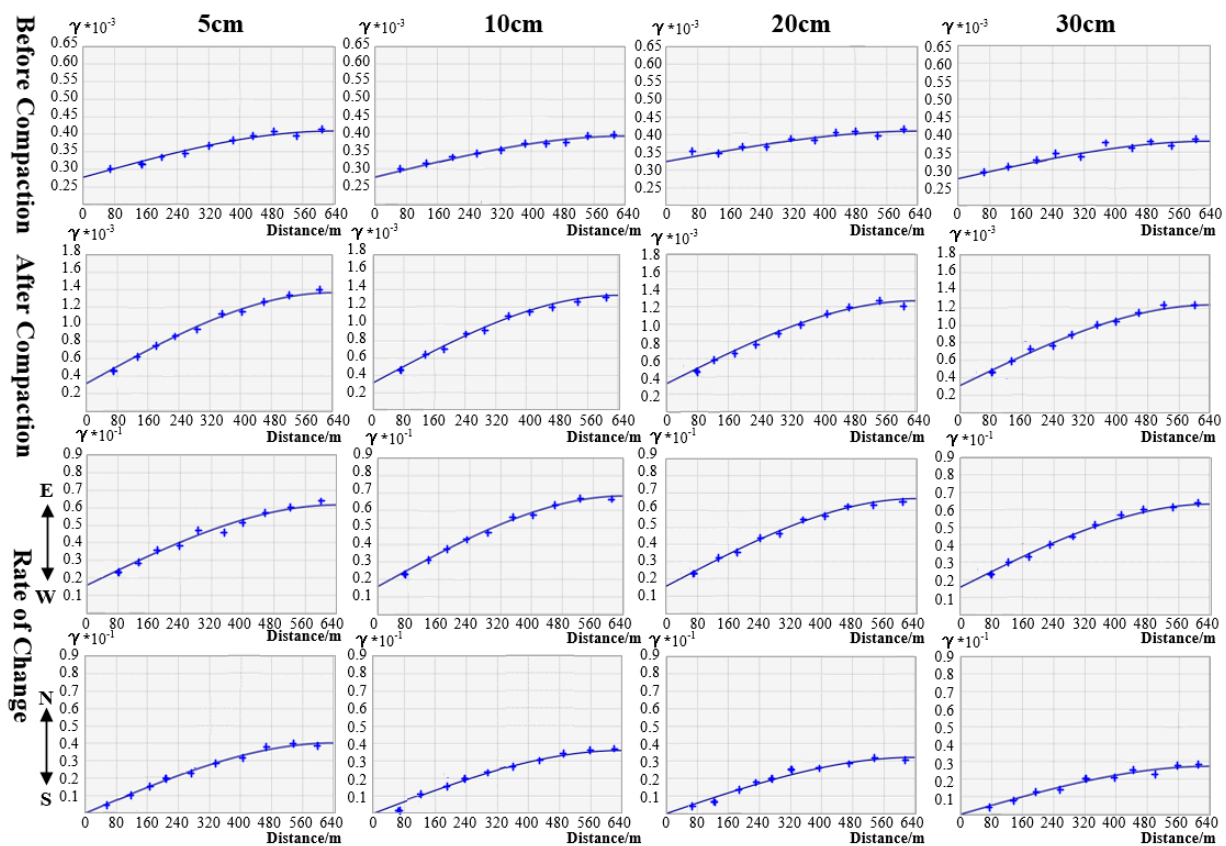


Figure 11. Transverse spatial semi–variance function of soil moisture content at various depths before and after compaction.

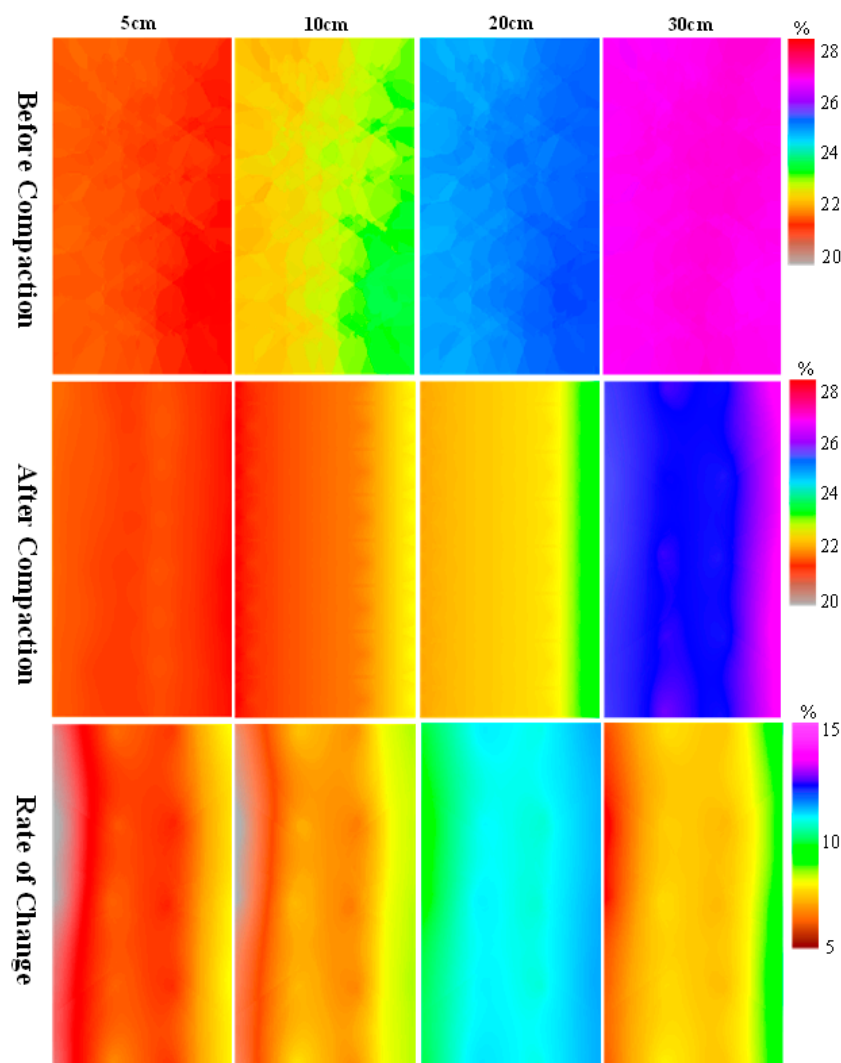


Figure 12. Transverse spatial distribution of soil moisture content at each depth before and after compaction.

The literature [20] investigated the spatial interpolation of soil moisture using different methods such as inverse distance weighting (IDW), ordinary kriging interpolation (Kriging), radial basis function interpolation (RBF) and regression kriging (RK) and compared the different results of the different interpolation methods. The spatial variability of soil moisture was analyzed. The literature [21] used RS and GIS spatial techniques for soil moisture prediction, and initially visualized soil moisture forecasting in a spatial context. In this study, ordinary kriging interpolation was used to analyze not only the longitudinal spatial variability but also the lateral spatial variability of soil water content over a large area of farmland.

5.2.3. The Effect of Tillage Compaction on the Spatial Lateral Variability of Soil Porosity in the Cultivated Layer

Figure 13 shows the transverse spatial semi-variance function of soil porosity at each depth before and after compaction. The ratios of block gold value to abutment $c_0/(c_0 + c)$ in the semi-variance function before the operation of each depth tillage layer were 80.5%, 77.6%, 68.9% and 75.7%, except for the 20 cm depth, which was greater than 75% but very close to 75% at 20 cm, so the spatial autocorrelation of the soil water content of the farmland before compaction was weak. The overall spatial autocorrelation of the soil water content in the farmland before compaction was weak; the ratios of the block gold value to the

abutment in the spatial semi-variance function of soil porosity in the tillage layer at each depth after unit operation were 24.9%, 23.2%, 23.9% and 24.4%, which were significantly lower than those before unit operation, with the values of $c_0/(c_0 + c)$ along the east–west direction being 11.6%, 19.7%, 24.7% and 22.6%, and the $c_0/(c_0 + c)$ values along the north–south direction being 21.26%, 20.5%, 9.2% and 30.2%, respectively. Figure 14 shows the transverse spatial distribution of soil porosity at each depth of the cultivated layer before and after compaction. It can be seen that after compaction, the soil porosity at each depth of the farmland is evenly distributed transversely. With the increase in depth, the soil porosity gradually decreases, and the greater the compactness of the soil the lower the porosity. The two are obviously negatively correlated. From the rate of change before and after compaction, the most affected is the surface soil. The reduction in soil porosity at 30 cm is not so obvious, and the compaction effect of the soil becomes weaker as the soil depth increases. There is an obvious break between the rate of change of soil porosity in test areas 2 and 3, which means that the impact of the farm machinery on soil porosity is reduced when the driver works after a lunch break, indicating that soil porosity is also indirectly influenced by driver fatigue. Combined with the semi-variance function analysis, it can be seen that the spatial lateral variability of soil porosity in the tillage layer increases after the machine operation and that the spatial variability of soil porosity along the north–south direction is stronger than that along the north–east direction, except for the 20 cm depth of the tillage layer.

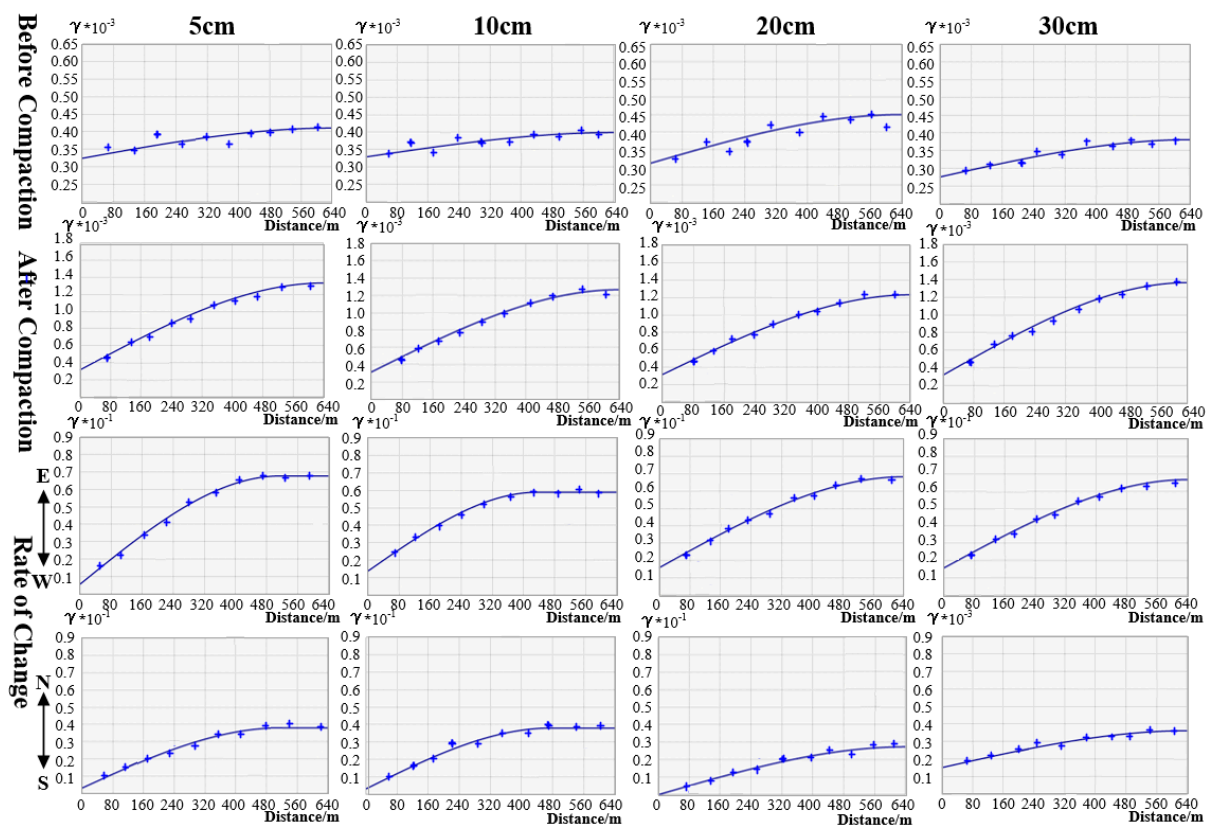


Figure 13. Transverse spatial semi–variance functions of soil porosity at various depths before and after compaction.

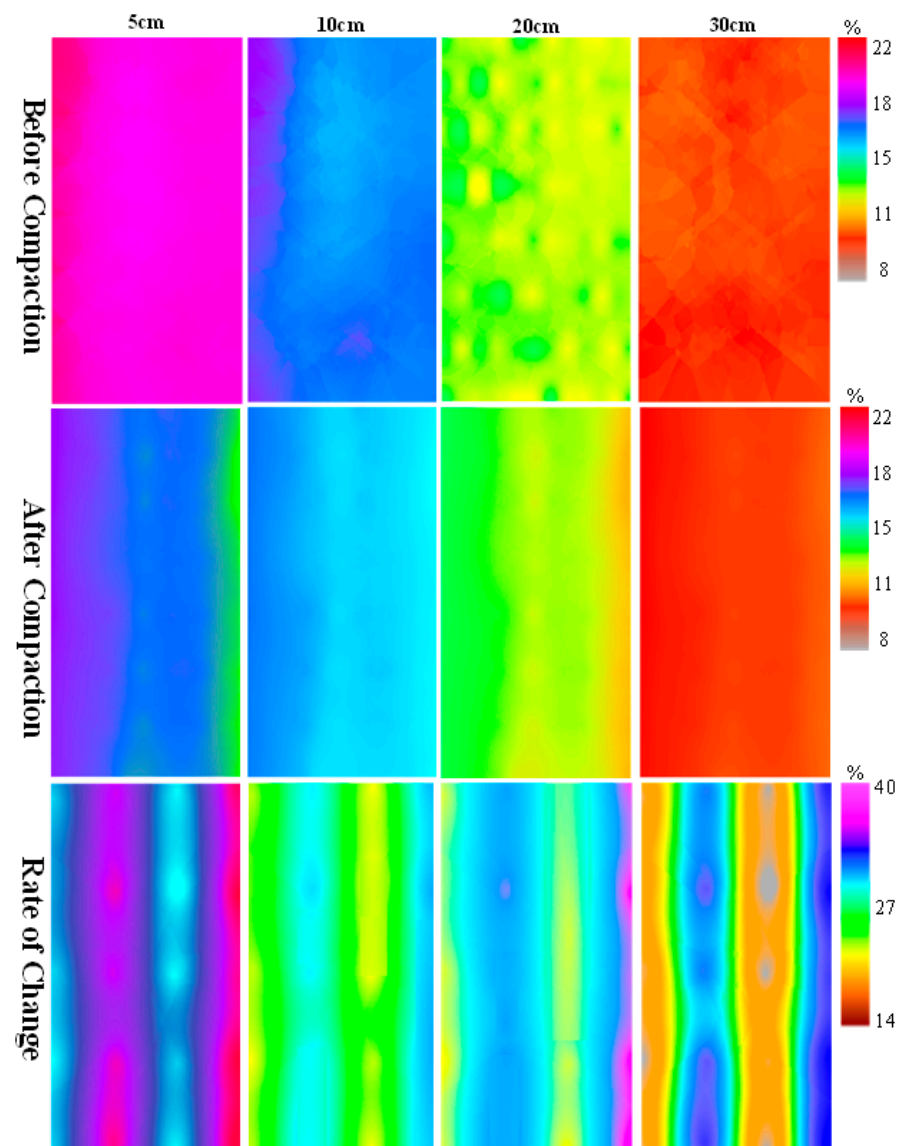


Figure 14. Lateral spatial distribution of soil porosity at each depth before and after compaction.

The literature [2] studied the effect of farmland traffic on soil, mainly analyzing the effect of tractor stress on soil porosity, and the results showed that when the number of compaction exceeds seven, a large additional soil stress is generated at a depth of 20–80 cm, resulting in a significant increase in soil porosity, which is in line with the results of this study, where the porosity of the soil surface layer increases significantly, but the study did not use the interpolation method to analyze the data. The literature [7] reviewed the research methods, technical characteristics and development trends in five key areas, including deep pine shovel design, drag resistance technology, tillage depth detection and control technology, and soil mechanical interaction research. Previous studies have mainly analyzed the compactness and capacity of the soil in the longitudinal direction. In this study, the kriging interpolation method was used to plot the semi-variance functions in the three directions of farmland, and a more detailed analysis of the spatial variability of farmland soil porosity was conducted.

6. Conclusions

- (1) The heavy-duty fertilizer-spreading unit had a significant compaction effect on the black soil layer, with the greatest change in compactness and porosity in the top-soil layer (at a 5 cm depth), where the rate of change in soil compactness reached 143.49%

and the rate of change in soil porosity reached 40.57%. The maximum variation in the water rate was reached at a depth of approximately 20 cm with a maximum value of 13.78%.

- (2) The results of the analysis of the longitudinal spatial variability show that, as shown in Table 4, the mean values of $c_0/(c_0 + c)$ for the spatial semi-variance functions of soil compactness, moisture content and porosity of the tillage layer in each test area before compaction were approximately 15%, 19% and 20%, respectively, and after compaction the mean values were approximately 33%, 23% and 30%, respectively, which indicates that compaction by high-power and no-tillage multifunction units leads to a reduction in the longitudinal spatial variability of soil physical parameters in the black soil layer. The mean values of $c_0/(c_0 + c)$ for the spatial semi-variance functions of soil compactness, moisture content and porosity variability of the tillage layer in each test area were approximately 24%, 14% and 12%, respectively, indicating that the effect of compaction by the heavy spreader unit on soil physical parameters was highly variable in the longitudinal space.
- (3) The results of the analysis of lateral spatial variability showed that, as shown in Table 4, the mean values of $c_0/(c_0 + c)$ of the spatial semi-variance functions of soil compactness, water content and porosity of the tillage layer at each depth before compaction were approximately 80%, 71% and 78%, respectively, and the mean values after compaction were approximately 40%, 23% and 24%, respectively, with the mean values of $c_0/(c_0 + c)$ along the east–west direction being approximately 8%, 27% and 18%, and the mean values of $c_0/(c_0 + c)$ along the north–south direction being approximately 9%, 0% and 20%. This indicates that compaction by the high-power and no-tillage multifunction units leads to increased lateral spatial variability of soil physical parameters in the cultivated layer at all depths of the black soil layer, with higher variability in the east–west space for soil physical compactness and porosity, and in the north–south direction for soil moisture content.

The findings of this study can provide a reference for future decisions on farming systems involving smart agriculture and environmentally friendly farm machinery, helping to achieve conservation tillage and eco-friendly agriculture.

Table 4. Values of $c_0/(c_0 + c)$ for the semi-variance function of soil parameters in the tillage layer before and after compaction.

Variable Name	Vertical $c_0/(c_0 + c)$			Horizontal $c_0/(c_0 + c)$			
	Before Compaction	Before Compaction	Rate of Change	Before Compaction	Before Compaction	After (E–W)	After (S–N)
Soil Compactness	15% Strong	33% Moderate	24% Strong	80% Weak	40% Moderate	8% Strong	9% Strong
Soil Water Content	19% Strong	23% Strong	14% Strong	71% Moderate	23% Strong	27% Moderate	0% Strong
Soil Porosity	20% Strong	30% Moderate	12% Strong	78% Weak	24% Strong	18% Strong	20% Strong

Author Contributions: Conceptualization, W.L.; data curation, W.L. and X.Y.; methodology, W.L. and W.G.; validation, W.L. and X.Y.; investigation, W.L. and Z.L.; resources, M.Y. and Z.S.; writing—original draft preparation, W.L.; writing—review and editing, W.L.; supervision, X.Y. and M.Y.; project administration, Z.S. and M.Y.; funding acquisition, X.Y. and Z.S. All authors have read and agreed to the published version of the manuscript.

Funding: This research was funded by the National Natural Science Foundation (No. 32201671), CCSA Science and Technology Think Tank Young Talent Program (No. 20220615ZZ07110119) and China Agricultural University 2115 Talent Engineering.

Acknowledgments: The authors would like to thank Jianshan Farm of the Great Northern Wilderness for providing the test plots.

Conflicts of Interest: The authors declare no conflict of interest.

References

1. Wang, X.; Wang, Q.; Li, H.; Li, W.; Niu, Q.; Chen, W. Effect of type induced soil compaction on soil properties and crop root growth under no-tillage system. *Trans. Chin. Soc. Agric. Mach.* **2017**, *48*, 168–175. [[CrossRef](#)]
2. Wang, X.; He, J.; Bai, M.; Liu, L.; Gao, S.; Chen, K.; Zhuang, H. The Impact of Traffic-Induced Compaction on Soil Bulk Density, Soil Stress Distribution and Key Growth Indicators of Maize in North China Plain. *Agriculture* **2022**, *12*, 1220. [[CrossRef](#)]
3. Qiang, X.; Sun, J.; Ning, H. Impact of Subsoiling on Cultivated Horizon Construction and Grain Yield of Winter Wheat in the North China Plain. *Agriculture* **2022**, *12*, 236. [[CrossRef](#)]
4. Acquah, K.; Chen, Y. Soil Compaction from Wheel Traffic under Three Tillage Systems. *Agriculture* **2022**, *12*, 219. [[CrossRef](#)]
5. Orzech, K.; Wanic, M.; Załuski, D. The Effects of Soil Compaction and Different Tillage Systems on the Bulk Density and Moisture Content of Soil and the Yields of Winter Oilseed Rape and Cereals. *Agriculture* **2021**, *11*, 666. [[CrossRef](#)]
6. Moitzi, G.; Sattler, E.; Wagentristl, H. Effect of Cover Crop, Slurry Application with Different Loads and Tire Inflation Pressures on Tire Track Depth, Soil Penetration Resistance and Maize Yield. *Agriculture* **2021**, *11*, 641. [[CrossRef](#)]
7. Lou, S.; He, J.; Li, H.; Wang, Q.; Lu, C.; Liu, W.; Liu, P.; Zhang, Z.; Li, H. Current Knowledge and Future Directions for Improving Subsoiling Quality and Reducing Energy Consumption in Conservation Fields. *Agriculture* **2021**, *11*, 575. [[CrossRef](#)]
8. Fu, X.; Shao, M. Improved Soil Sompaction Model and Experimental Study. *Trans. Chin. Soc. Agric. Eng. Trans. CSAE* **2007**, *23*, 1–5. [[CrossRef](#)]
9. Thomas, K. A Model for the Prediction of the Contact Area and the Distribution of Vertical Stress below Agricultural Tyres from Readily Available Tyre Parameters. *Biosyst. Eng.* **2005**, *92*, 85–96. [[CrossRef](#)]
10. Castioni, G.A.; de Lima, R.P.; Cherubin, M.R.; Bordonal, R.O.; Rolim, M.M.; Carvalho, L.N. Machinery traffic in sugarcane straw removal operation: Stress transmitted and soil compaction. *Soil Tillage Res.* **2021**, *213*, 105122. [[CrossRef](#)]
11. Obour, P.B.; Ugarte, C.M. A meta-analysis of the impact of traffic-induced compaction on soil physical properties and grain yield. *Soil Tillage Res.* **2021**, *211*, 105019. [[CrossRef](#)]
12. Faloye, O.T.; Ajayi, A.E.; Zink, A.; Fleige, H.; Dörner, J.; Horn, R. Effective stress and pore water dynamics in unsaturated soils: Influence of soil compaction history and soil properties. *Soil Tillage Res.* **2021**, *211*, 104997. [[CrossRef](#)]
13. Gemma, G.A. A Web-Enabled GIS Platform for Agricultural Land Use. IOP Conference Series Materials. *Sci. Eng.* **2020**, *803*, 012002. [[CrossRef](#)]
14. Yang, W.; Liao, H.; Pan, Z.; Li, X.; Li, T.; Li, J. Research on evaluation of suitability degree of industry transfer in gentle hillside Area in Chongqing based on GIS. *Trans. Chin. Soc. Agric. Eng. Trans. CSAE* **2015**, *31*, 244–252. [[CrossRef](#)]
15. Hu, Y.; Deng, L.; Zhang, S.; Ling, J.; Huang, S.; Kuang, X.; Liu, L. Changes of land use and landscape pattern in Xichang city based on RS and GIS. *Trans. Chin. Soc. Agric. Eng. Trans. CSAE* **2011**, *27*, 322–327. [[CrossRef](#)]
16. Liu, D.; Peng, L.; Gao, L.; Liu, J.; Sheng, L. Geographic information system (GIS)-based zoning of the suitability of *Dendrobium ferruginum* cultivation in Yunnan Province. *Trans. Jiangsu Agric. Sci.* **2017**, *45*, 227–230. [[CrossRef](#)]
17. Sun, H.; Wei, X.; Liu, W.; Li, D.; Jia, F.; Chen, N.; Sun, X. Evaluation method of cuacreslative effect of soil heavy metal ecological risk based on GIS baseline segmentation and land use unit optimization. *Trans. Geol.* **2022**, *96*, 1488–1502. [[CrossRef](#)]
18. John, B.; Das, S. Identification of risk zone area of declining piezometric level in the urbanized regions around the City of Kolkata based on ground investigation and GIS techniques. *Groundw. Sustain. Dev.* **2020**, *11*, 100354. [[CrossRef](#)]
19. Abuzaid, A.S.; AbdelRahman, M.A.E.; Fadl, M.E.; Antonio, S. Land Degradation Vulnerability Mapping in a Newly-Reclaimed Desert Oasis in a Hyper-Arid Agro-Ecosystem Using AHP and Geospatial Techniques. *Agronomy* **2021**, *11*, 1426. [[CrossRef](#)]
20. Zhang, Y.; Wang, J.; Zhang, J. Study on Interpolation Method of Soil Moisture based on GIS and Statistical Models. *Trans. J. Sichuan Norm. Univ. (Nat. Sci.)* **2019**, *42*, 703–710. [[CrossRef](#)]
21. Liu, Y.; Ye, C.; Wang, K. Soil moisture prediction technique in Beijing supported by RS and GIS techniques. *Trans. Chin. Soc. Agric. Mach.* **2008**, *24*, 155–160. [[CrossRef](#)]
22. Qaio, J.; Zhang, D.; Zhang, H.; Zhang, B.; Chen, H.; Chen, L.; Zheng, D.; Sun, J. Effects of soil compaction by various tractors on soil pene tration resistance and soybean yields. *Trans. Chin. Soc. Agric. Eng. Trans. CSAE* **2019**, *35*, 26–33. [[CrossRef](#)]